ORGANOMETALLICS

Article

pubs.acs.org/Organometallics

2,6-Diisopropylphenylamides of Potassium and Calcium: A Primary Amido Ligand in s-Block Metal Chemistry with an Unprecedented Catalytic Reactivity

Carsten Glock,[†,§] Fadi M. Younis,[†,§] Steffen Ziemann,[†] Helmar Görls,[†] Wolfgang Imhof,[‡] Sven Krieck,[†] and Matthias Westerhausen*[,†]

[†]Institut für Anorganische und Analytische Chemie, Friedrich-Schiller-Universität Jena, Humboldtstrasse 8, D-07743 Jena, Germany

[‡]Institut für Integrierte Naturwissenschaften, Abteilung Chemie, Universität Koblenz-Landau, Universitätsstrasse 1, D-56070 Koblenz, Germany

Supporting Information

ABSTRACT: Transamination of $KN(SiMe_3)_2$ with 2,6-diisopropylphenylamine (2,6-diisopropylaniline) in toluene at ambient temperature yields $[K\{N(H)Dipp\}\cdot KN(SiMe_3)_2]$ (**1**) regardless of the applied stoichiometry. Recrystallization of **1** in the presence of tetramethylethylenediamine (TMEDA) and tetrahydrofuran (THF) leads to the formation of $[(\mu\text{-thf})K_2\{N(H)Dipp\}_2]_\infty$ (**2**), whereas potassium bis(trimethylsilyl)amide remains in solution. Addition of pentamethyldiethylenetriamine (PMDETA) gives $[(pmdeta)K\{N(H)Dipp\}]_2$ (**3**). In contrast to the thf and pmdeta adducts, which lead to dissociation of **1** into homoleptic species, addition of bidentate dimethoxyethane maintains the mixed complex $[(dme)K\{\mu\text{-}N(SiMe_3)_2\}\{\mu\text{-}N(H)Dipp\}K]_2$ (**4**). A complete transamination of 2,6-diisopropylaniline with $KN(SiMe_3)_2$ in toluene at 100 °C yields $[K\{N(H)Dipp\}]$ (**5**), which reacts with CaI_2 to give $[(thf)_nCa\{N(H)Dipp\}_2]$ (**6**), $[(pmdeta)Ca\{N(H)Dipp\}_2]$ (**7**), and $[(dme)_2Ca\{N(H)Dipp\}_2]$ (**8**), depending on the solvents and coligands. Excess potassium 2,6-diisopropylphenylamide allows the formation of the calciate $[K_2Ca\{N(H)Dipp\}_4]_\infty$ (**9**). Hydroamination of diphenylbutadiyne with 2,6-diisopropylaniline in the presence of catalytic amounts of **9** gives tetracyclic 2,6-diisopropyl-9,11,14,15-tetraphenyl-8-azatetracyclo[8.5.0.0^{1,7}.0^{2,13}]pentadeca-3,5,7,9,11,14-hexaene (**10**). Solid-state structures are reported for **2**−**4** and **7**−**10**. Compound **10** slowly rearranges to tetracyclic 5a,9-diisopropyl-2,3,10,11-tetraphenyl-5a,6-dihydro-2a^1,6-ethenocyclohepta[*cd*]isoindole (**11**), which is slightly favored according to quantum chemical studies.

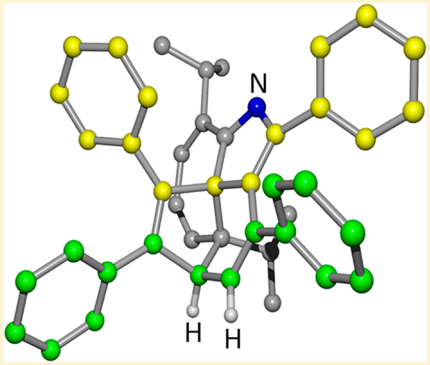

INTRODUCTION

Substituted amides of the electropositive s-block metals represent valuable reagents for diverse applications such as metalation, transamination, and amide transfer. Whereas several reviews exist discussing structures, properties, and reactivity of alkali-metal amides,[1] interest in organyl-substituted alkaline-earth-metal bis(amides) has been limited mainly to magnesium derivatives for a long time.[2] The homologous heavier alkaline-earth-metal complexes have attracted attention only for about the last two decades.[3,4] Early attempts gave insoluble, poorly characterized, and partially pyrophoric alkaline-earth-metal amides.[5] Approximately 20 years ago, the breakthrough succeeded with the synthesis of the alkaline-earth-metal bis[bis(trialkylsilyl)amides], which are soluble in common organic solvents such as ethers and aromatic and aliphatic hydrocarbons, allowing homogeneous reaction conditions.[6]

In recent years the portfolio of amides of the heavy alkaline-earth metals Ae became versatile. Solubility was guaranteed by substitution of only one trialkylsilyl group of $Ae\{N(SiMe_3)_2\}_2$ by an aryl substituent, leading to substituted trimethylsilylanilides.[3,7] Recently also diphenylamides[8] and *N*-alkylanilides[9] have been prepared and structurally characterized. In contrast to these complexes, which are soluble in tetrahydrofuran (THF), the 2,2,6,6-tetramethylpiperidylcalcium complexes express an enormous reactivity and cannot be handled in THF because of ether degradation processes.[9] In contrast to the case for stable amidomagnesium halides these Hauser-type bases of calcium show ligand redistribution processes (Schlenk-type equilibrium) favoring homoleptic calcium bis(amide) and calcium dihalide.[10]

Primary anilides of the heavier alkaline-earth metals tend to form aggregates (Ca) or even polymers (Sr, Ba) in the solid state and are only sparingly soluble in Lewis basic donor solvents.[11] 2,6-Difluoroanilides form more soluble complexes, but fluorine substituents in metal organic compounds may be hazardous and decompose spontaneously and violently.[12] *o*-Alkyl-substituted anilides form monomeric complexes with a strongly Lewis basic coligand such as hexamethylphosphoric acid triamide (hmpa), and mononuclear complexes of the type $[(hmpa)_3Ae\{N(H)Dipp\}_2]$ (Dipp = C_6H_3-2,6-iPr$_2$) were isolated.[3]

Received: February 21, 2013
Published: April 16, 2013

   dx.doi.org/10.1021/om4001007 | *Organometallics* 2013, 32, 2649−2660

Scheme 1. Reaction Scheme for the Synthesis of Potassium, Calcium, and Mixed-Metal 2,6-Diisopropylanilides

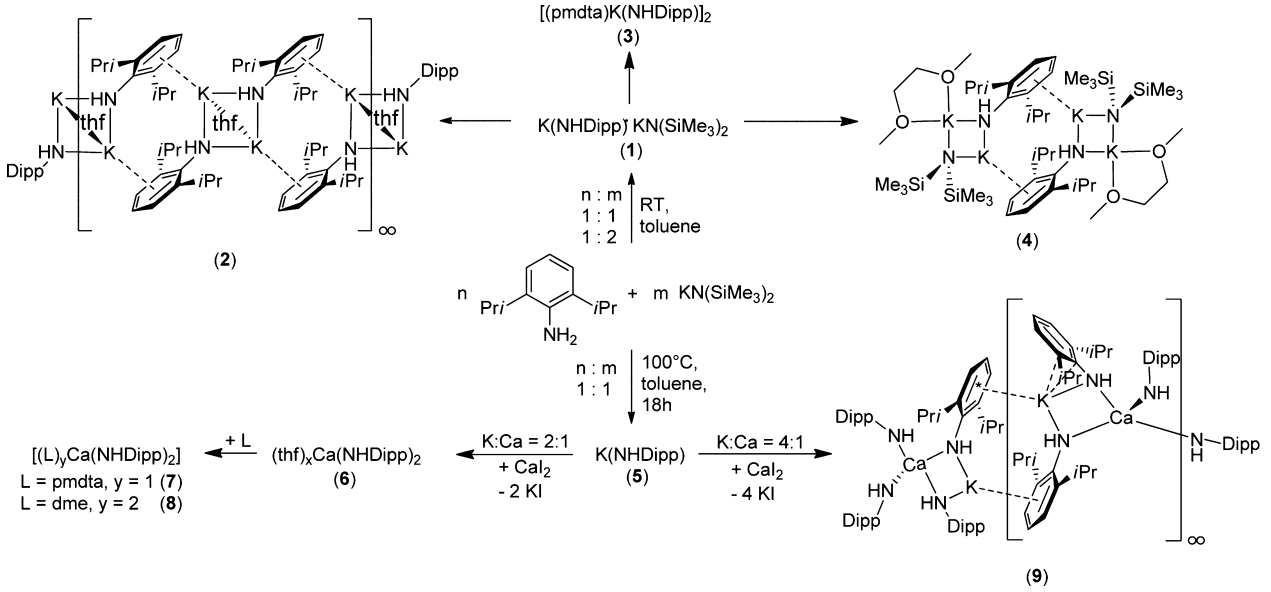

Heterobimetallic s-block metal amides exhibit significantly enhanced reactivity. Mixed alkali-metal−magnesium amides tend to form inverse crowns which react as highly reactive metalation reagents,[13] whereas the alkali-metal−calcium derivatives can best be described as alkali-metal calciates due to the amido transfer from the alkali metal to calcium.[9,14−16]

The awakened interest in these alkaline-earth-metal amides is also based on the catalytic activity (for recent general reviews see ref 17) in hydroamination reactions of carbodiimides,[18] alkenes,[19,20] and alkynes.[16,20] Especially calcium is a very attractive inexpensive element, due to its worldwide availability and nontoxicity regardless of the concentration. In many catalytic applications Ae$\{N(SiMe_3)_2\}_2$ was employed as the precatalyst, intermediately forming the catalytically active calcium amides. We could demonstrate that often highly reactive heterobimetallic compounds such as potassium calciates are required to catalyze the addition of amines to carbon−carbon multiple bonds.[16]

RESULTS AND DISCUSSION

Synthesis. Transamination of $KN(SiMe_3)_2$ with 2,6-diisopropylphenylamine (H_2N-Dipp) in toluene at room temperature led to precipitation of $[K\{N(H)Dipp\}\cdot KN(SiMe_3)_2]$ (**1**) regardless of the applied stoichiometry. The formation of a solid precipitate impeded the complete conversion to potassium 2,6-diisopropylphenylamide. Addition of Lewis bases often yields smaller and soluble aggregates which allow spectroscopic characterization. Compound **1** was dissolved in a mixture of tetramethylethylenediamine (TMEDA) and tetrahydrofuran (THF), and from this solution crystals of $[(\mu\text{-thf})K_2\{N(H)Dipp\}_2]_\infty$ (**2**) precipitated, whereas potassium bis(trimethylsilyl)amide remained in solution (Scheme 1). A similar finding was observed upon addition of a solvent mixture of pentamethyldiethylenetriamine (PMDETA) and THF, yielding crystalline $[(pmdeta)K\{N(H)Dipp\}]_2$ (**3**), whereas $KN(SiMe_3)_2$ remained in the mother liquor. In contrast to the thf and pmdeta adducts, which led to dissociation of **1** into homoleptic species, addition of bidentate 1,2-dimethoxyethane (DME) maintained the mixed stoichiometry and tetranuclear $[(dme)K\{\mu\text{-}N(SiMe_3)_2\}\{\mu\text{-}N(H)Dipp\}\text{-}K]_2$ (**4**) was isolated.

More drastic reaction conditions during transamination of $KN(SiMe_3)_2$ with H_2N-Dipp gave solvent-free $K\{N(H)Dipp\}$ (**5**), which was used as an amide transfer reagent. The metathesis reaction of this potassium amide with calcium diiodide yielded the oily substance $[(thf)_nCa\{N(H)Dipp\}_2]$ (**6**) in solvents such as THF, hexane, toluene, and mixtures thereof. The addition of tridentate pmdeta or bidentate dme led to crystalline $[(pmdeta)Ca\{N(H)Dipp\}_2]$ (**7**) and $[(dme)_2Ca\{N(H)Dipp\}_2]$ (**8**), respectively. Excess potassium 2,6-diisopropylphenylamide yielded the calciate $[K_2Ca\{N(H)Dipp\}_4]_\infty$ (**9**), which precipitated from a THF solution as a solvent-free coordination polymer.

The influence of the metals on the chemical ^1H and $^{13}C\{^1H\}$ NMR shifts of the 2,6-diisopropylphenylamide ions is small and seems to be not especially diagnostic of structure. Therefore, a detailed discussion is not included and the data are given in the Supporting Information. 2,6-Diisopropylaniline shows low-field-shifted ^1H NMR resonances of the aryl and amino hydrogen atoms. For the potassium derivatives these signals are high-field-shifted; however, the values of the calcium complexes are very similar. The tertiary CH fragments of the isopropyl groups show chemical shifts of δ 3.15 and 3.00 for the potassium and calcium anilides, respectively.

In the $^{13}C\{^1H\}$ NMR spectra the largest differences are observed for the ipso-carbon atoms; deprotonation of 2,6-diisopropylaniline leads to a significant low-field shift. The formation of heterobimetallic potassium tetrakis(anilido)-calciate shifts the resonance of the ipso-carbon back toward a higher field. The influences of the metal and the environment of the amido functionality (terminal or bridging position) on the other carbon atoms are very small, and no dependency is observed for the chemical shifts of the isopropyl groups.

On the basis of NMR parameters structure elucidation is impossible. All s-block metal amides **1**−**9** show only one set of resonances with very similar chemical shifts. This finding is in agreement with the expectation that in ionic amides the nature of the metal atoms plays an ancillary role. Dissociation of these complexes and fast dynamic behavior on the NMR time scale

dx.doi.org/10.1021/om4001007 | Organometallics 2013, 32, 2649−2660

(thus breaking up polymeric structures) explain not only this observation but also solubility in common organic donor solvents. Due to the fact that information on solution structures is very limited, we investigated the solid-state structures in order to verify the formation of homometallic and mixed s-block metal amides and to study the influence of coordinated solvent molecules.

Molecular Structures. Schematic representations are given in Scheme 1, and the molecular structures of the potassium amides **2**–**4**, and the calcium bis(anilides) **7** and **8** as well as the coordination polymer **9** are discussed in detail.

The molecular structure and numbering scheme of a section of polymeric **2** are shown in Figure 1. The central structural

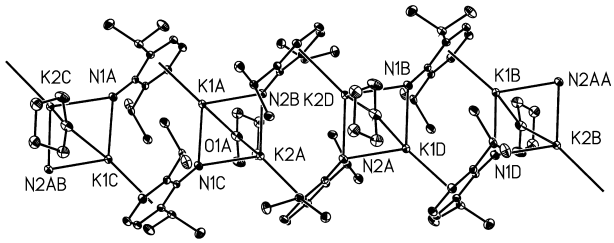

Figure 1. Section of polymeric **2**. The ellipsoids represent a probability of 40%, and H atoms are neglected for clarity. Symmetry-related atoms are marked with the letters A–D. Selected bond lengths (pm): K1A–N1C = 277.9(2), K1A–N2B = 275.4(2), K1A–O1A = 294.7(2), K2A–N1C = 277.3(2), K2A–N2B = 275.2(2), K2A–O1A = 286.8(2), K1A–C1A = 318.2(2), K1A–C2A = 316.7(2), K1A–C3A = 314.8(2), K1A–C4A= 313.3(2), K1A–C5A = 313.3(2), K1A–C6A = 317.3(2), K2A–C13A = 315.0(2), K2A–C14A = 322.0(2), K2A–C15A = 320.9(2), K2A–C16A = 314.4(2), K2A–C17A = 306.8(2), K2A–C18A = 306.6(2), N1C–C1C = 135.6(2), N2B–C13B = 135.8(2).

fragment consists of a four-membered K_2N_2 ring (average K–N distance 276.4 pm) with a bridging thf ligand between the potassium atoms. Thus, there exist three bridges between the alkali-metal atoms, leading to a short K1···K2 contact of only 349.1(1) pm. The dinuclear units are aligned to a one-dimensional strand via Lewis acid–base interactions between the soft potassium cations and the π systems of neighboring anilide moieties.

Enhancing the denticity and base strength of the neutral coligand allows the isolation of molecular dinuclear potassium anilides. The molecular structure and numbering scheme of **3** are displayed in Figure 2. The central structural fragment is the centrosymmetric planar four-membered K_2N_2 ring with different K–N bond lengths of 279.4(3) and 291.6(3) pm. The shorter K–N distance belongs to an interaction between K1 and an sp^2 hybrid orbital of N1, whereas the other potassium shows a more side-on coordination to the anilide anion (p_z orbital at N1), leading also to rather short contacts to C1 (314.8(3) pm) and C6 (329.3(3) pm). The nonbonding trans-annular K1···K1A contact adopts a rather large value of 421.1(1) pm. The coordination sphere of potassium is saturated by nitrogen bases of the pmdeta ligand, which shows two short K–N bonds (289.2(3) and 296.9(3) pm) and one significantly larger K–N distance of 318.3(3) pm.

The central four-membered K_2N_2 ring is also formed for heteroleptic $[(dme)K\{\mu\text{-}N(SiMe_3)_2\}\{\mu\text{-}N(H)Dipp\}K]_2$ (**4**), which is shown in Figure 3. The bulky bridging bis(trimethylsilyl)amide anions together with bidentate 1,2-dimethoxyethane hinder the formation of a one-dimensional

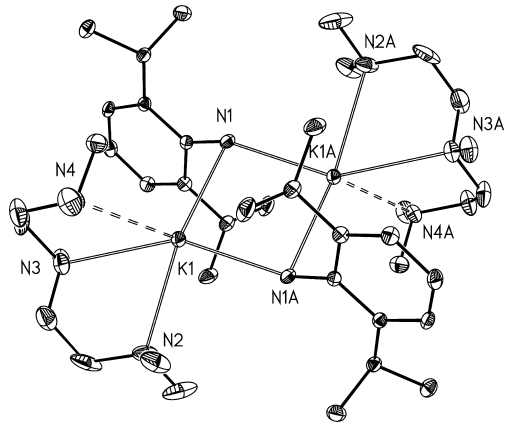

Figure 2. Molecular structure and numbering scheme of **3**. The ellipsoids represent a probability of 40%, and H atoms are omitted for clarity. The symmetry-equivalent half of the molecule ($-x + 2, -y, -z + 1$) is marked with the letter A. Selected bond lengths (pm): K1–N1 = 291.6(3), K1–N1A = 279.4(3), K1–N2 = 289.2(3), K1–N3 = 296.9(3), K1–N4 = 318.3(3), N1–C1 = 136.3(4).

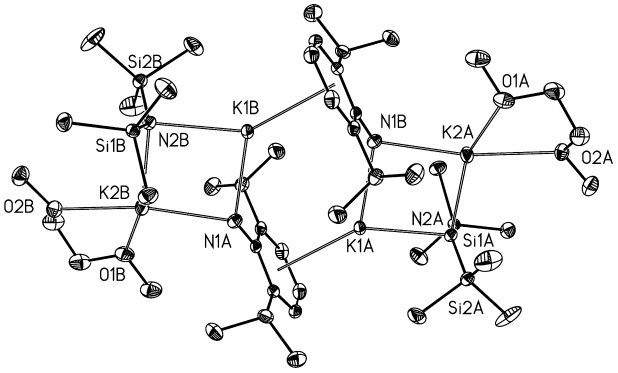

Figure 3. Molecular structure and numbering scheme of **4**. The ellipsoids represent a probability of 40%, and H atoms are neglected. The symmetry-related molecule halves ($-x + 2, -y + 1, -z$) are distinguished by the letters A and B. Selected bond lengths (pm): K1A–N1B = 274.2(1), K1A–N2A = 280.9(1), K2A–N1B = 276.3(1), K2A–N2A = 274.3(1), K2A–O1A = 273.3(1), K2A–O2A = 276.2(1), K1A–C1A = 320.3(1), K1A–C2A = 326.2(1), K1A–C3A = 323.5(2), K1A–C4A = 318.9(2), K1A–C5A = 315.3(2), K1A–C6A = 316.1(1), N1A–C1A = 135.9(2), N2A–Si1A = 166.8(1), N2A–Si2A = 166.8(1).

coordination polymer. Instead, two dinuclear units are interconnected by contacts between the potassium atoms and the π systems of the aryl groups. The highly ionic nature of the K–N interactions leads to strong electrostatic attractions between the nitrogen atom and the silicon atoms and, hence, short Si–N2 bonds of 166.8(1) pm due to back-donation of charge from the nitrogen atom to the silyl groups (hyperconjugation into σ^*(Si–C) bonds). The short N2–Si bonds enforce a large Si1–N2–Si2 bond angle of 133.43(8)° due to repulsive forces between the bulky trimethylsilyl groups. A similar effect was already discussed for dimeric $[KN(SiMe_3)_2]_2$.[21]

Crystalline monomeric 2,6-diisopropylanilides of calcium were obtained with multidentate coligands such as pmdeta and dme, yielding $[(pmdeta)Ca\{N(H)Dipp\}_2]$ (**7**) and $[(dme)_2Ca\{N(H)Dipp\}_2]$ (**8**), respectively. The molecular structure and numbering scheme of **7** is displayed in Figure 4. The pentacoordinate calcium atom binds to two anilide anions

dx.doi.org/10.1021/om4001007 | Organometallics 2013, 32, 2649–2660

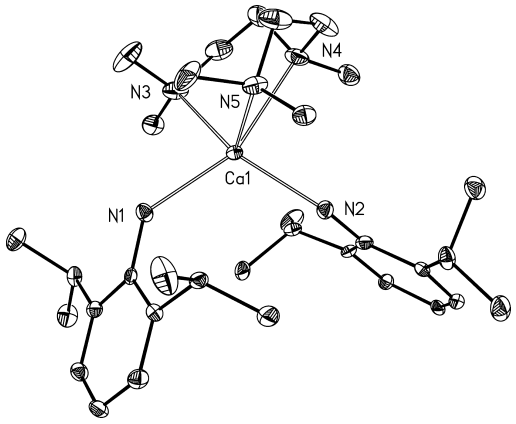

Figure 4. Molecular structure and numbering scheme of **7**. The ellipsoids represent a probability of 40%, and H atoms are not drawn. Selected bond lengths (pm): Ca1−N1 = 232.4(4), Ca1−N2 = 229.2(5), Ca1−N3 = 259.5(5), Ca1−N4 = 258.0(5), Ca1−N5 = 255.2(5), N1−C1 = 137.5(6), N2−C13 = 137.0(6). Selected bond angles (deg): N1−Ca1−N2 = 112.9(2), Ca1−N1−C1 = 136.7(3), Ca1−N2−C13 = 146.1(4).

and a tridentate pmdeta ligand. Due to additional electrostatic attraction the Ca1−N1 and Ca1−N2 distances to the anilides are more than 20 pm smaller than those to the pmdeta base. In addition, the small bite of the nitrogen bases of the pmdeta ligand (N···N distances) leads to very small N3−Ca1−N4 and N4−Ca1−N5 bond angles of 70.4(2) and 72.3(2)°. A rather small N1−Ca1−N2 bond angle of 112.9(2)° is enabled because the Ca1−N−C angles of the anilide ligands are widened to 136.7(3)° for N1 and 146.1(4)° for N2.

The complex $[(dme)_2Ca\{N(H)Dipp\}_2]$ (**8**) crystallizes in the centrosymmetric triclinic space group with four molecules A−D in the asymmetric unit. The molecular structure and numbering scheme of molecule A is represented in Figure 5. The hexacoordinate calcium atom is located in a significantly distorted octahedral environment due to small bites of the dme ligands and widened N−Ca−N angles. The larger coordination number of 6 leads to lengthened Ca−N bonds in comparison

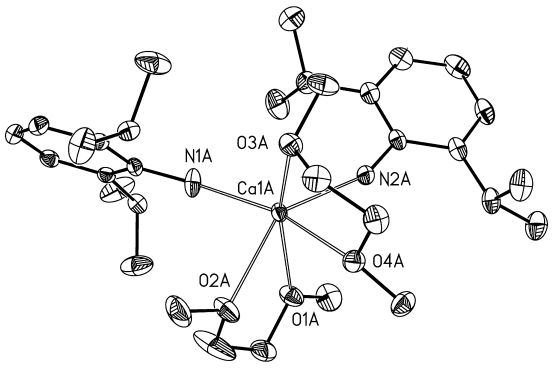

Figure 5. Molecular structure and numbering scheme of **8**. The ellipsoids represent a probability of 40%, and H atoms are omitted for clarity reasons. The asymmetric unit contains four molecules A−D; only molecule A is depicted. Selected bond lengths (pm): Ca1A−N1A = 230.6(4), Ca1A−N2A = 231.6(4), Ca1A−O1A = 242.5(3), Ca1A−O2A = 249.6(4), Ca1A−O3A = 242.8(3), Ca1A−O4A = 249.7(3), N1A−C1A = 136.9(5), N2A−C13A = 138.0(5). Selected bond angles (deg): N1A−Ca1A−N2A = 115.2(2), Ca1A−N1A−C1A = 156.8(3), Ca1A−N2A−C13A = 157.0(3).

to complex **7**. The N−Ca−N angles for the molecules A−D vary significantly and are larger for A, B, and D despite a larger coordination number (molecule A, 115.2(2)°; molecule B, 117.6(1)°; molecule C, 88.6(1)°; molecule D, 122.3(1)°), whereas molecule C deviates from the other molecules and a very small value is observed. Intramolecular strain leads to strongly widened Ca−N−C angles, and the four molecules show different values (molecule A, 156.8(3) and 157.0(3)°; molecule B, 137.0(3) and 154,6(3)°; molecule C, 147.5(3) and 149.6(3)°; molecule D, 159.2(3) and 137.4(3)°). The flexibility of the Ca−N−C angles supports the chemical intuition that electrostatic and steric forces dominate the structure and that covalent Ca−N bond contributions play insignificant roles.

In heterobimetallic amides the less electropositive metal commonly binds to the amido ligands, forming a metalate, whereas the more electropositive metal represents the counter-cation. We included the heterobimetallic amide with a potassium to calcium ratio of 2:1 in our structural investigations because mixed-metal amides often behave differently than the homometallic congeners.[13,14] The K to Ca ratio of 2:1 justifies considering this derivative as a higher order calciate. Therefore, the structure of the calciate $[K_2Ca\{N(H)Dipp\}_4]_\infty$ (**9**) was determined and a section of the coordination polymer is displayed in Figure 6. The calcium atom is in a distorted-

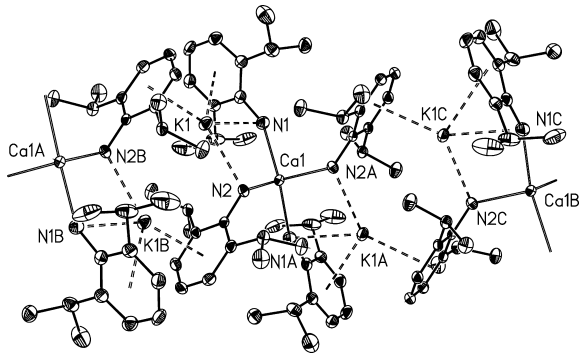

Figure 6. Section of the polymeric structure of **9**. The ellipsoids represent a probability of 40%, and H atoms are neglected for clarity . The letters A (−*x*, *y*, −*z* + 0.5) and B (−*x*, −*y* + 2, −*z*) characterize symmetry-related atoms. Selected bond lengths (pm): Ca1−N1 = 232.9(3), Ca1−N2 = 239.3(3), K1−N1 = 294.1(3), K1−C1 = 292.9(3), K1−N2 = 287.2(3), K1−C13B = 335.0(3), K1−C14B = 324.1(3), K1−C15B = 308.8(3), K1−C16B = 304.2(4), K1−C17B = 312.1(3), K1−C18B = 327.4(3), N1−C1 = 137.9(4), N2−C13 = 137.9(4). Selected bond angles (deg): N1−Ca1−N2 = 100.3(1), N1−Ca1−N1A = 152.4(2), N1−Ca1−N2A = 98.6(1), N2−Ca1−N2A = 93.2(1), Ca1−N1−C1 = 155.8(3), Ca1−N1−K1 = 90.5(1), Ca1−N2−C13 = 127.0(2), Ca1−N2−K1 = 90.93(9).

tetrahedral environment with N−Ca−N angles between 93.2(1) and 153.4(2)°. Despite the small coordination number of 4, rather large Ca−N bond lengths of 232.9(3) and 239.3(3) pm are observed due to electrostatic repulsion between the amide anions and intramolecular steric strain between the bulky aryl groups of neighboring amido ligands. The flexibility of the Ca−N−C bond angles (155.8(3) and 127.0(2)°) again supports the mainly ionic nature of this compound. These tetrakis(anilido)calciates are interconnected by potassium countercations that bind to the nitrogen atoms (K−N = 287.2(3) and 294.1(3) pm) and saturate their coordination sphere by Lewis acid−base interactions to the π systems of the aryl groups. The remarkable reactivity can be understood on

dx.doi.org/10.1021/om4001007 | *Organometallics* 2013, 32, 2649−2660

Table 1. Average Bond Lengths (pm) of Selected Amides of Potassium and Calcium as Well as Their Mixed-Metal Derivatives[a]

compd	av Ca−N	av K−N	av Ca−L	av K−L	ref
		Potassium Amides			
$[KN(SiMe_3)_2]_2$		278.7			21
$[(tmeda)KTmp]_2$		279.2		295.1 (N)	22
$[(thf)_3KNPh_2]_2$		282.6		272.0 (O)	23
$[(pmdeta)KNPh_2]_2$		282.9		292.2 (N)	24
$[(pmdeta)KN(iPr)Ph]_2$		289.1		297.7 (N)	24
$[(dme)_2KN(iPr)Ph]_2$		287.3		286.8 (O)	24
$[(pmdeta)KN(H)Dipp]_2$		285.5		301.5 (N)	this work
$[(diox)_{1.5}KNPh_2]_\infty$		284.6		270.7 (O)	25
$[(tmeda)_{1.5}KNPh_2]_\infty$		287.4		290.5 (N)	26
$[\{KN(Me)Ph\}_3]_\infty$		282.4			24
$[\{(thf)_{0.5}KN(iPr)Ph\}_2]_\infty$		279.7		276.3 (O)	24
$[\{(thf)KN(iPr)Ph\}_5]_\infty$		280.8		272.9 (O)	24
$[(dme)_{0.25}KN(iPr)Ph]_\infty$		281.0		278.1 (O)	24
$[(thf)KN(H)Dipp]_\infty$		276.4		290.7 (O)	this work
		Calcium Amides			
$[(thf)_2Ca\{N(SiMe_3)_2\}_2]$	230.2		237.7 (O)		27
$[(dme)Ca\{N(SiMe_3)_2\}_2]$	227.1		239.7 (O)		28
$[(tmeda)Ca\{N(SiMe_3)_2\}_2]$	231.5		259.2 (N)		10
$[(tmeda)Ca(Tmp)_2]$	227.5		264.5 (N)		9
$[(tmeda)Ca\{N(iPr)_2\}_2]$	227.2		260.2 (N)		10
$[(dme)_2Ca(NPh_2)_2]$	236.9		246.1 (O)		8
$[(thf)_4Ca\{N(Me)Ph\}_2]$	241.5		240.7 (O)		12
$[(thf)_3Ca\{N(iPr)Ph\}_2]$	234.9		242.7 (O)		9
$[(thf)_2Ca\{N(SiMe_3)Dipp\}_2]$	232.6		235.6 (O)		7c
$[(thf)_2Ca\{N(SiMe_3)Mes\}_2]$	230.4		234.3 (O)		7b
$[(tmeda)Ca\{N(SiMe_3)Mes\}_2]$	231.1		252.9 (N)		7b
$[(dme)_2Ca\{N(H)Dipp\}_2]$	231.1		246.2 (O)		this work
$[(pmdeta)Ca\{N(H)Dipp\}_2]$	230.8		257.6 (N)		this work
		Potassium Calciates			
$[(thf)_4K_2Ca\{N(iPr)Ph\}_4]$	241.8			268.7	9
$[(tmeda)_2K_2Ca\{N(iPr)Ph\}_4]$	244.1	294.6		283.7	15
$[(thf)_3K_2Ca(NPh_2)_4]_\infty$	240.3			265.2	9
$[K_2Ca\{N(H)Dipp\}_4]_\infty$	236.1	290.7			Tthis work

[a]Abbreviations: diox, 1,4-dioxane; Dipp, 2,6-diisopropylphenyl; dme, 1,2-dimethoxyethane; L, neutral Lewis base such as ethers and amines; Me, methyl; Mes, 2,4,6-trimethylphenyl; Ph, phenyl; pmdeta, pentamethyldiethylenetriamine; Pr, propyl; thf, tetrahydrofuran; tmeda, tetramethylethylenediamine; Tmp, 2,2,6,6-tetramethylpiperidide.

the basis of a small coordination number of calcium (accessibility of calcium by the substrate) and of electrostatic repulsion between the anilide anions (enhancing the nucleophilicity and availability of the anilide anions) in addition to increased nucleophilicity caused by the electron-donating isopropyl groups.

Selected structural parameters of potassium and calcium amides are compared in Table 1. The amides of the heavier alkali metals and alkaline-earth metals have attracted tremendous interest because they react as highly reactive nucleophiles and metalation reagents as well as hydroamination catalysts.[17] The reactivity can be adjusted with the s-block metals potassium and calcium or even by employing their heterobimetallic derivatives. Due to a larger size of the potassium ion and its smaller charge, the Ca−N bonds are generally significantly shorter than the K−N bonds. Small variations depend on the coordination number of the s-block metals and on the bulkiness of the amides and coligands. In solvent-depleted compounds, the potassium ions also form strong bonds to the π systems of aryl groups, whereas solvent-free calcium amides dimerize via bridging amido ligands.[28] This π-philicity of the potassium ion was already investigated in detail at benzyl alkali-metal solvates;[29] whereas lithium and sodium ions show the shortest distances to the methylene unit, the potassium ion prefers a side-on coordination to the aromatic π system of the phenyl group. This finding supports the notion that the potassium ion represents a significantly softer cation than the lighter congeners and the doubly charged calcium ions. In heterobimetallic amides of potassium and calcium, the amido anions always bind to the harder divalent calcium ion, forming tetrakis(amido)calciates with tetracoordinate calcium centers. Due to the concentration of negative charge in the vicinity of calcium, neutral Lewis bases such as thf and tmeda bind at potassium. If the neutral coligands have weak coordination properties toward K^+ ions in comparison to the π systems of the phenyl groups, interactions between the potassium ion and the π systems of aryl substituents are operative, often leading to aggregation and formation of coordination polymers.

Hydroamination of Diphenylbutadiyne. Hydroamination is an atom-economic process for the preparation of substituted amines. However, thermodynamic and kinetic challenges aggravate the direct nucleophilic attack of the amine at an electron-rich C−C multiple bond. In addition, the large energy difference between the N−H and the C−C

dx.doi.org/10.1021/om4001007 | Organometallics 2013, 32, 2649−2660

multiple bond and entropic effects are disadvantageous. Therefore, activation of the C−C multiple bond (by side-on coordination to transition metals) or of the amine (amide or imide formation at electropositive metals and lanthanoids) is required.

Intermolecular hydroamination of diphenylbutadiyne with diphenylamine required a very reactive catalyst.[16,20] Whereas the reactivity of the diphenylamides of potassium and calcium were insufficient to mediate this hydroamination reaction, catalytic amounts of heterobimetallic $[K_2Ca(NPh_2)_4]$ led to the formation of singly hydroaminated diphenylbutadiyne.[16] In contrast to this finding, the more nucleophilic *N*-isopropylanilides of potassium and of calcium are able to mediate the hydroamination of diphenylbutadiyne with *N*-isopropylaniline. The potassium-mediated hydroamination of diphenylbutadiyne with *N*-isopropylaniline gave small amounts of the side product 1-isopropylphenylamino-2,4-bis(phenylethynyl)-3-phenylnaphthalene with a 2:1 stoichiometry of diphenylbutadiyne to aniline.[16]

Hydroamination of butadiynes yielding pyrroles succeeds via a copper(I)-catalyzed addition of aniline to diphenylbutadiyne (Scheme 2).[30] Another strategy for the synthesis of pyrroles

Scheme 2. Copper(I)-Mediated Synthesis of Pyrroles via Double Hydroamination of Diphenylbutadiyne with Aniline

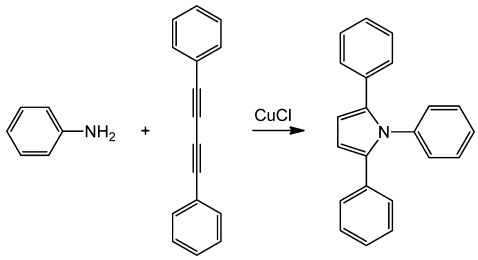

was developed via the titanium-mediated double hydroamination of 1,4-pentadiynes with primary amines.[31] If benzylamine was used in these catalytic hydroamination reactions, pyridine derivatives were obtained.[30−32] Here we investigated the calcium-mediated hydroamination of diphenylbutadiyne with 2,6-diisopropylaniline. A single hydroamination would yield 1,4-diphenyl-1-(2,6-diisopropylanilino)-but-1-ene-3-yne, and a second intramolecular hydroamination step could allow the isolation of *N*-2,6-diisopropylphenylpyrrole. However, the hydroamination of diphenylbutadiyne with primary 2,6-diisopropylaniline proceeded surprisingly different in the presence of catalytic amounts of **9**. Similarly to the observation of the formation of the naphthalene side product,[16] 1 equiv of aniline reacted with 2 equiv of butadiyne, as shown in Scheme 3, regardless of the applied stoichiometry. In Figure 7 the color code clarifies the origin of the building blocks (black and blue, C and N of 2,6-diisopropylaniline; yellow and green, two diphenylbutadiyne units). This compound cocrystallized with half a diphenylbutadiyne molecule.

The resulting crystalline tetracyclic imine, 2,6-diisopropyl-9,11,14,15-tetraphenyl-8-azatetracyclo[8.5.0.0^{1,7}.0^{2,13}]-pentadeca-3,5,7,9,11,14-hexaene (**10**), was obtained with a yield of 82%. The formation of this product does not depend on the reaction temperature and succeeded in boiling THF and at ambient temperature; only the reaction period was extended at lower temperatures.

Scheme 3. Calciate-Mediated Hydroamination of Diphenylbutadiyne with 2,6-Diisopropylaniline in Tetrahydrofuran, Yielding Tetracyclic Imine 10[a]

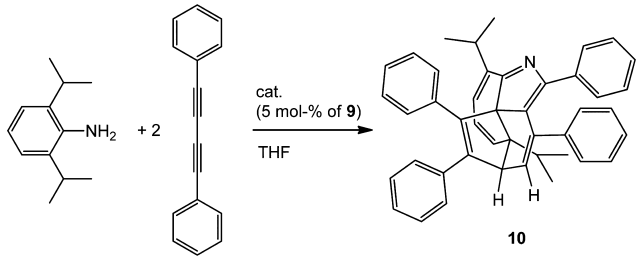

[a]See text and Figure 7.

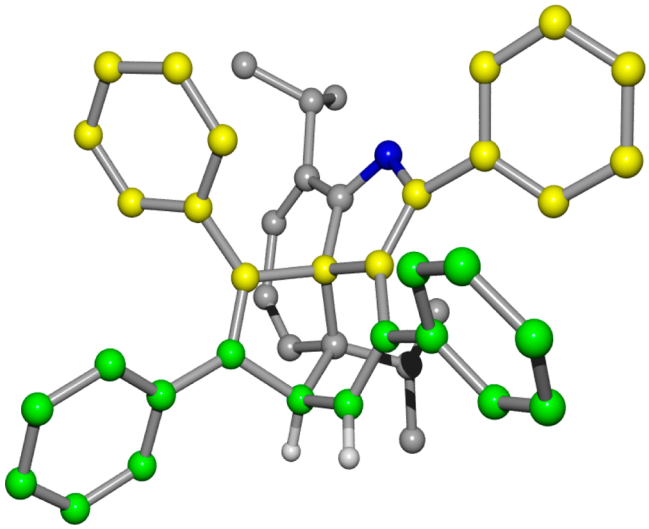

Figure 7. Ball-and-stick model of 2,6-diisopropyl-9,11,14,15-tetraphenyl-8-azatetracyclo[8.5.0.0^{1,7}.0^{2,13}]pentadeca-3,5,7,9,11,14-hexaene (**10**), clarifying the building blocks of this tetracyclic compound (black and blue, C and N of 2,6-diisopropylaniline; yellow and green, two diphenylbutadiyne units). The H atoms (light gray) are neglected, with the exception of those stemming from the aniline.

The molecular structure of **10** is displayed in Figure 8. The labeling of the atoms shows the numbering in accordance with the chemical name for the inner tetracyclic unit, with the nitrogen atom N8 being in position 8. For the numbering of the substituents, the digit of the adjacent ring atom was expanded by an additional digit to distinguish the carbon atoms within a substituent.

The nitrogen atom N8 is bound in a five-membered ring with a C7═N8 double bond and a N8−C9 single bond of 131.2(2) and 141.8(2) pm, respectively. From these values it is obvious that there is no significant delocalization within the conjugated system. A vast steric strain is introduced at the C1 atom, which is a member of all four cycles. This fact leads to severe deviations from a tetrahedral environment (C−C1−C values deviate from 101.2(1) to 120.3(2)°) toward a trigonal-pyramidal environment[33] and to a significant elongation of the C1−C bonds. The adjacent C2 atom even shows stronger deviations from ideal tetrahedral symmetry. The smallest C1−C2−C13 angle shows a value of only 95.7(1)° between three sp^3-hybridized carbon atoms and a C2−C13 bond length of 157.5(2) pm. Distortions also widen the angles at the vicinal diphenylethene fragment with C15−C14−C141 and C14−C15−C151 values of 129.9(2) and 130.1(2)°, respectively.

dx.doi.org/10.1021/om4001007 | *Organometallics* 2013, 32, 2649−2660

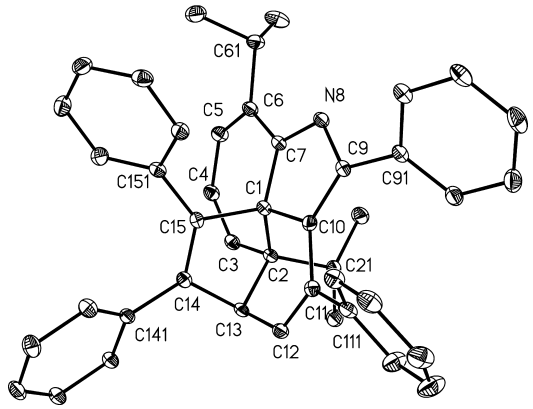

Figure 8. Molecular structure and numbering scheme of **10**. The ellipsoids represent a probability of 40%, and all H atoms are omitted for clarity. Selected bond lengths (pm): C1−C2 = 156.2(2), C1−C7 = 150.2(2), C1−C10 = 151.6(2), C1−C15 = 154.8(2), C2−C3 = 150.4(3), C2−C21 = 155.2(3), C3−C4 = 134.1(3), C4−C5 = 145.7(3), C5−C6 = 135.2(3), C6−C7 = 144.4(3), C6−C61 = 152.4(3), C7−N8 = 131.2(2), N8−C9 = 141.8(2), C9−C10 = 136.6(3), C9−C91 = 147.9(3), C10−C11 = 145.0(2), C11−C12 = 135.5(3), C11−C111 = 149.0(3), C12−C13 = 151.1(3), C13−C14 = 153.3(3), C14−C15 = 134.2(3), C14−C141 = 147.5(2), C15−C151 = 147.7(3).

Initially it was astonishing that tetracyclic imine **10** with three chiral carbon atoms formed in such a selective manner. The proposed reaction mechanism is presented in Scheme 4, offering two feasible pathways. The first reaction step is the addition of an anilide to the triple bond of diphenylbutadiyne, yielding **A**. Another alkyne inserts into the newly formed metal−carbon bond (carbometalation step to **B**). Thereafter, an intramolecular metalation yields amide **C** with a metal−nitrogen bond. The very nucleophilic amido base forms an imine, and cyclization leads to the formation of the 1,2,4,6-cycloheptratetraene derivative **D** with the negative charge at the 5-position (exemplified in Scheme 4 by an M−C bond). This carbanion reacts with H_2N-Dipp, thus regenerating the 2,6-diisopropylanilido catalyst M{N(H)Dipp} and leading to intermediate metal-free **E**. The 1,2,4,6-cycloheptratetraene fragment is very reactive, due to ring strain caused by the ketene moiety. Therefore, a cyclization reaction releases this strain and annihilates the aromatic character of the Dipp group, resulting in the tricyclic derivative **F**. Strained 1,2,4,6-cycloheptatetraenes have already attracted much interest and were prepared and preserved in an argon matrix.[34] Isomeric $C(CH)_6$ was intensively investigated by quantum chemical methods as free molecules[35] as well as a hydrocarbon captured in a molecular container.[36] These investigations show that 1,2,4,6-cycloheptatetraene is favored in comparison to a carbene embedded in a seven-membered ring.

An alternative pathway allows the protonation of **C** (and, hence, the formation of amine **G**, which is shown here with a collinear arrangement of the alkyne units requiring a specific isomerism at the C=C double bonds) combined with the re-formation of the anilido catalyst (Scheme 4). Thereafter, a Bergman cyclization leads to the formation of the diradical species **H**, which also rearranges to the tricyclic imine **F**, accompanied by a hydrogen abstraction from the amino functionality. This hydrogen transfer from the amino unit to the carbon atom is accompanied by C−C bond formation, leading to a breakup of the aromaticity of the Dipp group. The thermally controlled Bergman cyclization reactions of non-conjugated (*Z*)-hexa-1,5-diyne-3-ene yields *p*-benzyne with a triplet ground state,[37] whereas photochemically induced cyclizations follow other pathways.[38] The Bergman cyclization can be triggered by heat[39] and by internal amide functionalities,[40] occasionally also metal-mediated.[41]

A final rearrangement step yields tetracyclic 2,6-diisopropyl-9,11,14,15-tetraphenyl-8-azatetracyclo[8.5.0.0^{1,7}.0^{2,13}]-pentadeca-3,5,7,9,11,14-hexaene (**10**; 5a,9-diisopropyl-2,3,10,11-tetraphenyl-5,5*a*-dihydro-2a^1,5-ethenocyclohepta[*cd*]-isoindole), containing three chiral carbon atoms at positions 1, 2, and 13. The driving force of this final reorganization of the molecule, which divides the π system into a shorter conjugated unit (C3−C12) and an isolated C14=C15 double bond, is release of steric strain between the isopropyl group at C2 and the phenyl group at C15 (which are oriented to opposite sides of molecule **10**) as well as between neighboring phenyl substituents. Due to the strained tetracyclic structure only two enantiomers were observed and characterized by X-ray crystallography and NMR studies in order to verify the proposed structure.

During extensive NMR investigations of **10** it was observed that new resonances developed within a few days that finally grew to an approximate equimolar ratio with starting 7,15-diisopropyl-2,3,10,12-tetraphenyl-9-azatetracyclo-[8.5.0.0^{1,7}.0^{2,13}]pentadeca-3,5,7,9,11,14-hexaene (**10**). A complete conversion to 5a,9-diisopropyl-2,3,10,11-tetraphenyl-5a,6-dihydro-2a^1,6-ethenocyclohepta[*cd*]isoindole (**11**) and also purification efforts have failed as of yet. Therefore, the structure of the rearrangement product **11** was derived from NMR spectra and DFT calculations. A rearrangement mechanism is proposed in Scheme 5. This rearrangement breaks and forms a C−C bond and rearranges the conjugated π system; however, the number and size of rings as well as double bonds remain unchanged in the resulting **11**, suggesting solely reduction of intramolecular strain as the driving force for this rearrangement. Consequently the energy difference between **10** and **11** is rather small, with **11** being favored by 17.46 kJ mol^{-1} according to DFT calculations. A comparison of experimental and calculated NMR data (Table 2; for assignments see Scheme 6) shows slightly low field shifted resonances. Nevertheless, experimental parameters are in accordance with the calculated values. The trends are expressed correctly, clearly supporting the above suggested interpretation of the experimental findings.

In order to support the proposed reaction mechanisms and to deduce the importance of steric strain for the rearrangement step from **F** to **10** and from **10** to **11**, quantum chemical investigations were performed.

Quantum Chemical Investigations. Total energies E_{corr} with thermal and entropic corrections being applied as well as the number of imaginary frequencies are summarized in Table 3. We started our investigations on a simplified unsubstituted model (marked with "_**H**"; Scheme 4, R = R′ = H). Here derivative **F_H** is favored by 64.5 kJ mol^{-1} in comparison to the 1,2,4,6-cycloheptatetraene intermediate **E_H**. Surprisingly, the derivative **F_H** also is 60.5 kJ mol^{-1} lower in energy than **10_H** without isopropyl and phenyl groups. Due to the fact that unsubstituted **11_H** is only 17.4 kJ mol^{-1} lower in energy than **10_H**, derivative **F_H** represents the thermodynamically most stable product: i.e., in theory the calciate-mediated reaction of aniline with butadiyne might well end with the formation of **F_H**.

dx.doi.org/10.1021/om4001007 | *Organometallics* 2013, 32, 2649−2660

Scheme 4. Proposed Mechanism for the Calciate-Mediated Formation of Imine 10[a]

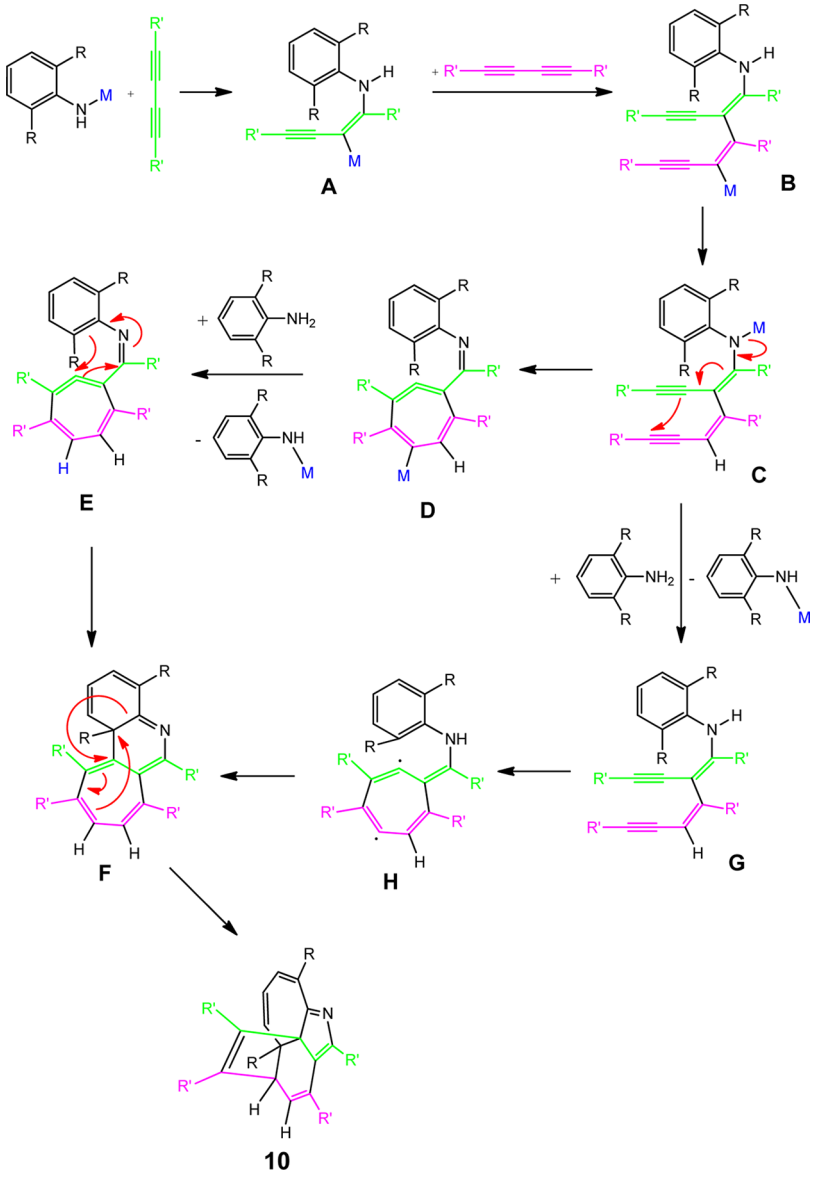

[a]R = *i*Pr, R′ = Ph; see text.

Scheme 5. Rearrangement of 10, Yielding 5a,9-Diisopropyl-2,3,10,11-tetraphenyl-5a,6-dihydro-2a^1,6-ethenocyclohepta[*cd*]isoindole (11)

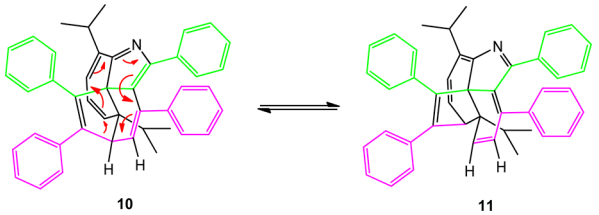

Taking the substituents into account (designated with "_S"; R = *i*Pr, R′ = Ph), the situation changes significantly. In the final rearrangement from **10_S** to **11_S** the situation is similar to that for the unsubstituted derivatives, with product **11_S** again being favored by 17.6 kJ mol^{-1}. However, the substituted molecule **F_S** does not represent a minimum structure, due to massive intramolecular strain between neighboring phenyl groups. Optimization of **F_S** leads to the highly endothermic formation of an intermediate in which the neighboring phenyl substituents performed a formal [2 + 2] cycloaddition reaction, which is not a productive reaction pathway in the context of the experimentally observed reaction. Therefore, **F_S** cannot be considered as an intermediate in the formation of tetracyclic **10_S** and **11_S** but might be considered as a transition state. Moreover, the substituted intermediate **E_S** is energetically favored by 13.3 kJ mol^{-1} in comparison to **10_S** and is only 4.3 kJ mol^{-1} less stable than substituted **11_S**. The latter nevertheless is the thermodynamically most stable isomer if the substituted derivatives are considered. The alternative pathway via intermediate **G_S** is feasible from a theoretical point of view because substituted **G_S** is 48.2 kJ mol^{-1} higher in energy than **10_S**. In summary, the substitution pattern dramatically disadvantages intermediate **F_S**, although the unsubstituted derivative **F_H** represents the favored molecule if phenyl and isopropyl groups are neglected. Hence, the reaction

dx.doi.org/10.1021/om4001007 | *Organometallics* 2013, 32, 2649−2660

Table 2. Comparison of Experimental and Calculated $^{13}C\{^1H\}$ NMR Shifts of the Central Tetracyclic Units of 10 and 11[a]

10		11	
exptl	DFT	exptl	DFT
181.0	185	170.0	174
146.2	156	160.4	168
140.3	153	137.7	145
139.2	146	136.4	144
138.9	145	135.9	142
136.2	145	133.9	142
135.6	144	131.7	141
131.6	140	131.3	141
127.5	134	127.4	138
126.8	134	127.2	138
125.5	130	126.9	133
77.8	83	66.5	72
72.8	82	57.7	64
58.3	67	48.6	58

[a]The assignment of the chemical shifts is depicted in Scheme 6.

Scheme 6. Calculated ^1H (Chemical Shifts δ, left) and ^{13}C NMR Data (Right) of 10 (Top Row) and 11 (Bottom Row)

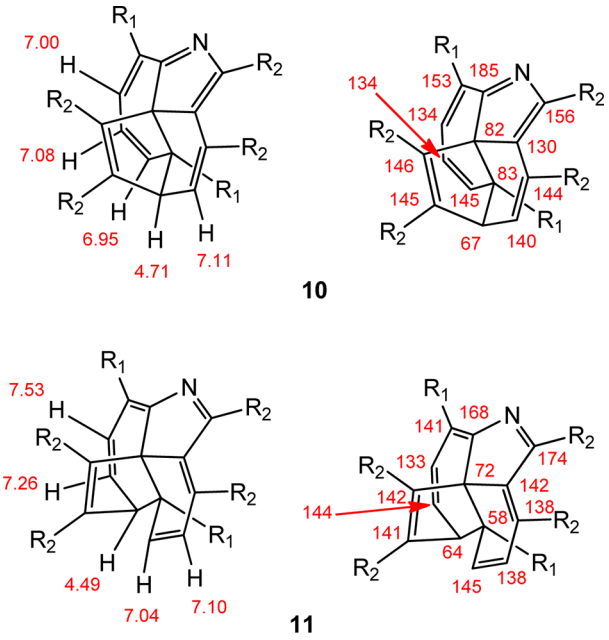

Table 3. Calculated Energies and Numbers of Imaginary Frequencies

compd[a]	E_{corr} (au)	N_{Imag}
E_H	−594.722615	0
E_S	−1754.647508	0
F_H	−594.747172	0
G_H	−594.695420	0
G_S	−1754.624103	0
10_H	−594.724130	0
10_S	−1754.642443	0
11_H	−594.730775	0
11_S	−1754.649164	0

[a]For all compounds denoted with the ending "_H", R = R′ = H; for all compounds denoted with the ending "_S", R = *i*Pr, R′ = Ph.

is pushed toward the tetracycle **10_S** in order to reduce intramolecular repulsion between adjacent phenyl groups.

CONCLUSION

Metalation of 2,6-diisopropylaniline with $K[N(SiMe_3)_2]$ yields the corresponding potassium salt $[K\{N(H)Dipp\}\cdot KN(SiMe_3)_2]$ (**1**), regardless of the applied stoichiometry. At elevated temperatures homoleptic $K\{N(H)Dipp\}$ (**5**) can be isolated. The aggregation degree of these potassium anilides strongly depends on the denticity of the neutral coligand. The addition of monobasic THF leads to polymeric $[(\mu\text{-thf})K_2\{N(H)Dipp\}_2]_\infty$ (**2**) in the solid state. Bidentate DME is able to stabilize tetranuclear $[(dme)K\{\mu\text{-}N(SiMe_3)_2\}\{\mu\text{-}N(H)Dipp\}K]_2$ (**4**), whereas in the presence of tridentate PMDETA dinuclear $[(pmdeta)K\{N(H)Dipp\}]_2$ (**3**) crystallizes. In all these solids the four-membered K_2N_2 ring is the dominating structural unit which can be interconnected via Lewis acid−base interactions between the soft potassium cations and the aryl π-systems.

These potassium anilides can be used as anilide transfer reagents. Thus, the metathetical approach with CaI_2 in tetrahydrofuran yields the corresponding calcium bis(2,6-diisopropylanilide) $[(thf)_nCa\{N(H)Dipp\}_2]$ (**6**), which can be purified and crystallized as monomeric and mononuclear complexes after addition of tri- and bidentate coligands such as pmdeta or dme, yielding $[(pmdeta)Ca\{N(H)Dipp\}_2]$ (**7**) and $[(dme)_2Ca\{N(H)Dipp\}_2]$ (**8**), respectively. Excess potassium 2,6-diisopropylphenylamide leads to the formation of the calciate $[K_2Ca\{N(H)Dipp\}_4]_\infty$ (**9**).

The potassium tetrakis(anilido)calciate **9** is highly reactive and enables a calciate-mediated hydroamination of diphenylbutadiyne with 2,6-diisopropylaniline. However, after this reaction step and a subsequent carbometalation of another butadiyne a reaction cascade leads to the formation of tetracyclic 2,6-diisopropyl-9,11,14,15-tetraphenyl-8-azatetracyclo-$[8.5.0.0^{1,7}.0^{2,13}]$pentadeca-3,5,7,9,11,14-hexaene (**10**), which slowly rearranges to 5a,9-diisopropyl-2,3,10,11-tetraphenyl-5a,6-dihydro-2a^1,6-ethenocyclohepta[*cd*]isoindole (**11**).

EXPERIMENTAL SECTION

General Remarks. All manipulations were carried out under an argon or a nitrogen gas atmosphere using standard Schlenk techniques. Solvents were dried according to common procedures and distilled under argon or nitrogen; deuterated solvents were dried with sodium, degassed, and saturated with an inert gas. $KN(SiMe_3)_2$ was purchased from Aldrich as a solid with a purity of 95% and used without further purification. Bruker AC 200, Bruker AC 400, and Bruker AC 600 spectrometers were used to record ^1H NMR and ^{13}C NMR spectra at ambient temperature in $[D_8]$THF solutions if no other solvent is mentioned. All spectra were referenced to deuterated THF as an internal standard. The anilido complexes were extremely sensitive toward moisture and air, and therefore, combustion analysis gave no reliable results.

Synthesis of K{N(H)Dipp}K{N(SiMe$_3$)$_2$} (1). $KN(SiMe_3)_2$ (2.15 g, 10.8 mmol) was dissolved in 22 mL of toluene and the solution filtered prior to use. To this clear, colorless solution was added H_2N-Dipp (1.0 mL, 5.3 mmol) via syringe with vigorous stirring at room temperature to yield a colorless precipitate of **1**. After 3 h of stirring, pure **1** was isolated by filtration, washed twice with 7.5 mL of toluene and finally with 10 mL of pentane, and then dried in vacuo. Yield: 2.05 g (4.9 mmol, 93%). ^1H NMR: δ 6.89 (2H, d, $^3J_{H,H}$ = 7.4 Hz, m-*H*), 5.84 (1H, t, $^3J_{H,H}$ = 7.4 Hz, p-*H*), 3.41 (1H, s, N*H*), 3.12 (2H, hept, $^3J_{H,H}$ = 6.8 Hz, C*H*), 1.16 (12H, d, $^3J_{H,H}$ = 6.8 Hz, CH_3), −0.19 (18H, s, $SiCH_3$). $^{13}C\{^1H\}$ NMR: δ 156.6 (*i*-*C*), 129.7 (*o*-*C*), 122.1 (*m*-*C*), 106.7 (*p*-*C*), 28.2 (CH), 23.1 ($iPrCH_3$), 6.4 ($SiCH_3$).

dx.doi.org/10.1021/om4001007 | *Organometallics* 2013, 32, 2649−2660

Synthesis of $[(\mu\text{-thf})K_2\{N(H)Dipp\}_2]_\infty$ (2). This approach was performed to yield a tmeda adduct. Therefore, **1** (256 mg, 0.6 mmol) was dissolved in 1.5 mL of a 2:1 mixture of TMEDA and THF, and this reaction mixture was heated to 60 °C. Crystalline **2** was obtained overnight from this solution at ambient temperature. ^{1}H NMR: δ 6.57 (4H, d, $^3J_{H,H}$ = 7.4 Hz, m-*H*), 5.81 (2H, t, $^3J_{H,H}$ = 7.4 Hz, p-*H*), 3.62 (thf), 3.45 (2H, s, N*H*), 3.15 (4H, hept, $^3J_{H,H}$ = 6.8 Hz, C*H*), 1.78 (thf), 1.17 (24H, d, $^3J_{H,H}$ = 6.8 Hz, CH_3). ^{13}C{^{1}H} NMR: δ 157.2 (*i*-*C*), 129.6 (*o*-*C*), 122.1 (*m*-*C*), 106.3 (*p*-*C*), 68.1 (thf), 28.3 (*C*H), 26.3 (thf), 23.3 (*C*H$_3$).

Synthesis of $[(pmdeta)K\{N(H)Dipp\}]_2$ (3). **1** (255 mg, 0.6 mmol) was dissolved in a mixture of 2 mL of PMDETA and 0.3 mL of THF, and this solution was heated to 60 °C. Standing at room temperature yielded crystalline needles of **3**. ^{1}H NMR: δ 6.56 (4H, d, $^3J_{H,H}$ = 7.4 Hz, m-*H*), 5.78 (2H, t, $^3J_{H,H}$ = 7.4 Hz, p-*H*), 3.39 (2H, s, N*H*), 3.15 (4H, hept, $^3J_{H,H}$ = 6.8 Hz, C*H*), 2.29−2.44 (*C*H$_2$-pmdeta), 2.19 + 2.15 (*C*H$_3$-pmdeta), 1.16 (24H, d, $^3J_{H,H}$ = 6.8 Hz, CH_3). ^{13}C{^{1}H} NMR: δ 157.9 (*i*-*C*), 129.5 (*o*-*C*), 122.1 (*m*-*C*), 105.8 (*p*-*C*), 58.8 + 57.3 (*C*H$_2$-pmdeta), 46.1 + 43.2 (*C*H$_3$-pmdeta), 28.3 (*C*H), 23.3 (*i*PrCH_3).

Synthesis of $[(dme)K\{\mu\text{-}N(SiMe_3)_2\}\{\mu\text{-}N(H)Dipp\}K]_2$ (4). **1** (316 mg, 0.8 mmol) was dissolved in 1 mL of DME. Subsequent cooling to 5 °C for about 1 week quantitatively resulted in crystalline **4**. ^{1}H NMR: δ 6.58 (4H, d, $^3J_{H,H}$ = 7.4 Hz, m-*H*), 5.83 (2H, t, $^3J_{H,H}$ = 7.4 Hz, p-*H*), 3.43 (2H, s, N*H*), 3.43 (*C*H$_2$-dme), 3.27 (*C*H$_3$-dme), 3.12 (4H, hept, $^3J_{H,H}$ = 6.8 Hz, C*H*), 1.16 (24H, d, $^3J_{H,H}$ = 6.8 Hz, CH_3), −0.19 (36H, s, Si*C*H$_3$). ^{13}C{^{1}H} NMR: δ 156.7 (*i*-*C*), 129.7 (*o*-*C*), 122.1 (*m*-*C*), 106.7 (*p*-*C*), 72.6 (*C*H$_2$-dme), 58.8 (*C*H$_3$-dme), 28.3 (*C*H), 23.2 (*i*PrCH_3), 6.5 (Si*C*H$_3$).

Synthesis of K{N(H)Dipp} (5). H$_2$N-Dipp (0.98 mL, 5.2 mmol) was added via syringe to a clear colorless solution of KN(SiMe$_3$)$_2$ (1.033 g, 5.2 mmol) in 15 mL of toluene. The resulting suspension was heated to 100 °C for 18 h, yielding an off-white powder of **5** that contains only trace amounts of the initial amide. Yield: 1.02 g (4.7 mmol, 91%). ^{1}H NMR: δ 6.55 (2H, d, $^3J_{H,H}$ = 7.4 Hz, m-*H*), 5.75 (1H, t, $^3J_{H,H}$ = 7.4 Hz, p-*H*), 3.36 (1H, s, N*H*), 3.16 (2H, hept, $^3J_{H,H}$ = 6.8 Hz, C*H*), 1.16 (12H, d, $^3J_{H,H}$ = 6.8 Hz, CH_3), −0.19 (1.2 H-equ, ∼7% Si*C*H$_3$). ^{13}C{^{1}H} NMR: δ 157.6 (*i*-*C*), 129.5 (*o*-*C*), 122.1 (*m*-*C*), 105.5 (*p*-*C*), 28.3 (*C*H), 23.3 (*i*PrCH_3), 6.5 (Si*C*H$_3$).

Synthesis of $[(thf)_xCa\{N(H)Dipp\}_2]$ (6). **5** (1.10 g, 5.1 mmol) and CaI$_2$ (0.75 g, 2.5 mmol) were dissolved in 15 mL of THF. Immediately, a white precipitate of KI formed that was separated by filtration over Celite after 2 h of stirring at room temperature. We note that no crystalline material could be obtained from this solution. Instead, **6** separated as an oil from diverse solvent mixtures (THF, toluene, hexane) during cooling.

Synthesis of $[(pmdeta)Ca\{N(H)Dipp\}_2]$ (7). A 3 mL portion of a THF solution of **6** was dried in vacuo. Redissolving in 5 mL of PMDETA and 1.75 mL of THF with heating followed by cooling to −20 °C overnight yielded colorless crystalline material. ^{1}H NMR: δ 6.63 (4H, d, $^3J_{H,H}$ = 7.4 Hz, m-*H*), 5.96 (2H, t, $^3J_{H,H}$ = 7.4 Hz, p-*H*), 3.31 (2H, s, N*H*), 3.00 (4H, hept, $^3J_{H,H}$ = 6.8 Hz, C*H*), 2.29−2.48 (*C*H$_2$-pmdeta), 2.20 + 2.16 (*C*H$_3$-pmdeta), 1.22 (24H, d, $^3J_{H,H}$ = 6.8 Hz, CH_3). ^{13}C{^{1}H} NMR: δ 156.9 (*i*-*C*), 130.4 (*o*-*C*), 122.1 (*m*-*C*), 108.7 (*p*-*C*), 58.8 + 57.3 (*C*H$_2$-pmdeta), 46.1 + 43.2 (*C*H$_3$-pmdeta), 29.4 (*C*H), 23.4 (*i*PrCH_3).

Synthesis of $[(dme)_2Ca\{N(H)Dipp\}_2]$ (8). Crystalline **8** was obtained when oily **6** was dissolved in a few milliliters of DME and cooled to −20 °C, yielding single crystals of **8**. ^{1}H NMR: δ 6.63 (4H, d, $^3J_{H,H}$ = 7.4 Hz, m-*H*), 5.96 (2H, t, $^3J_{H,H}$ = 7.4 Hz, p-*H*), 3.43 (*C*H$_2$-dme), 3.31 (2H, s, N*H*), 3.28 (*C*H$_3$-dme), 3.00 (4H, hept, $^3J_{H,H}$ = 6.8 Hz, C*H*), 1.22 (24H, d, $^3J_{H,H}$ = 6.8 Hz, CH_3). ^{13}C{^{1}H} NMR: δ 157.0 (*i*-*C*), 130.4 (*o*-*C*), 122.1 (*m*-*C*), 108.6 (*p*-*C*), 72.6 (*C*H$_2$-dme), 58.8 (*C*H$_3$-dme), 29.3 (*C*H), 23.4 (*i*PrCH_3).

Synthesis of $[K_2Ca\{N(H)Dipp\}_4]_\infty$ (9). **5** (814 mg, 3.8 mmol) and CaI$_2$ (280 mg, 0.9 mmol) were reacted in 10 mL of THF, and precipitation of finely divided KI was observed. THF-free crystalline material was obtained after reduction of the original volume of the calciate solution to one-third of its original volume, addition of 3 mL of toluene, and subsequent cooling to −20 °C for 2 weeks. ^{1}H NMR: δ 6.79 (8H, d, $^3J_{H,H}$ = 7.4 Hz, m-*H*), 6.31 (4H, t, $^3J_{H,H}$ = 7.4 Hz, p-*H*), 3.96 (4H, s, N*H*), 3.03 (8H, hept, $^3J_{H,H}$ = 6.8 Hz, C*H*), 1.20 (48H, d, $^3J_{H,H}$ = 6.8 Hz, CH_3). ^{13}C{^{1}H} NMR: δ 147.4 (*i*-*C*), 131.4 (*o*-*C*), 122.6 (*m*-*C*), 113.8 (*p*-*C*), 28.3 (*C*H), 23.0 (*i*PrCH_3).

Synthesis of 2,6-Diisopropyl-9,11,14,15-tetraphenyl-8-azatetracyclo[8.5.0.0^{1,7}.0^{2,13}]pentadeca-3,5,7,9,11,14-hexaene (10). Diphenylbutadiyne (0.51 g, 2.47 mmol) was dissolved in 12 mL of THF before 2,6-diisopropylaniline (0.23 mL, 1.26 mmol) and 5 mol % of the calciate **9** were added, and the mixture was stirred overnight. A standard workup procedure including hydrolysis with 15 mL of water, extraction with diethyl ether, drying with sodium sulfate, and recrystallization from pentane gave **10** as a crude product which contained half a molecule of diphenylbutadiyne per formula unit. Final purification was performed via gradient column chromatography over silica gel, starting with pure aliphatic hydrocarbons followed by a 1:1 mixture of alkanes and ethyl acetate. The residue was recrystallized from pentane at −20 °C, yielding orange **10** (0.60 g, 1.03 mmol, 82%). Mp: 122−125 °C. NMR data without phenyl groups are as follows (for assignment see Scheme 6). ^{1}H NMR (C$_6$D$_6$, 600 MHz, 295 K): δ 6.54 (1H, d, $^3J_{H,H}$ = 6.4 Hz), 6.24 (1H, dd, $^3J_{H,H}$ = 8.6 + 12.1 Hz), 6.14 (1H, d, $^3J_{H,H}$ = 8.6 Hz), 5.81 (1H, d, $^3J_{H,H}$ = 12.1 Hz), 3.96 (1H, d, $^3J_{H,H}$ = 6.4 Hz), 3.62 (1H, hept, $^3J_{H,H}$ = 6.9 Hz, C*H*-*i*Pr), 1.89 (1H, hept, $^3J_{H,H}$ = 6.9 Hz, C*H*-*i*Pr), 1.18 (3H, d, $^3J_{H,H}$ = 6.9 Hz, CH_3-*i*Pr), 0.81 (3H, d, $^3J_{H,H}$ = 7.0 Hz, CH_3-*i*Pr), 0.80 (3H, d, $^3J_{H,H}$ = 7.0 Hz, CH_3-*i*Pr), 0.52 (3H, d, $^3J_{H,H}$ = 6.8 Hz, CH_3-*i*Pr). ^{13}C{^{1}H} NMR (C$_6$D$_6$, 150 MHz, 295 K): δ 181.0, 146.2, 140.3, 139.2, 138.9, 136.2, 135.6, 131.6, 127.5, 126.8, 125.5, 77.8, 72.8, 58.3, 30.8, 30.8, 23.1, 22.3, 18.7, 17.7. Anal. Calcd for C$_{44}$H$_{39}$N (581.78): C, 90.84; H, 6.76; N, 2.41. Found: C, 90.80; H, 6.90; N, 2.40. MS (EI, *m*/*z* (%)): 581 (12) [M]$^+$, 379 (40) [M − diyne]$^+$, 202 (44) [diyne], 177 (100) [C$_{12}$H$_{19}$N]$^+$, 162 (68) [C$_{12}$H$_{17}$]$^+$. IR: 1599 w, 1491 w, 1443 w, 1261 m, 1177 w, 1056 w, 1027 m, 964 w, 917 w, 839 m, 756 s, 693 vs, 662 w, 608 w, 531 w, 417 w cm^{-1}.

Synthesis of 5a,9-Diisopropyl-2,3,10,11-tetraphenyl-5a,6-dihydro-2a^1,6-ethenocyclohepta[*cd*]isoindole (11). In solution product **10** rearranged with reduction of intramolecular steric strain, yielding **11**. Due to the fact that this compound always contained significant amounts of **10**, characterization was limited to NMR data. NMR parameters without phenyl groups are as follows (for assignment see Scheme 6). ^{1}H NMR (C$_6$D$_6$, 600 MHz, 295 K): δ 6.58 (1H, d, $^3J_{H,H}$ = 12.2 Hz), 6.53 (1H, d, $^3J_{H,H}$ = 9.5 Hz), 6.49 (1H, dd, $^3J_{H,H}$ = 7.6 + 12.2 Hz), 6.00 (1H, d, $^3J_{H,H}$ = 9.5 Hz), 4.64 (1H, hept, $^3J_{H,H}$ = 7.0 Hz, C*H*-*i*Pr), 3.91 (1H, d, $^3J_{H,H}$ = 7.5 Hz), 2.03 (1H, hept, $^3J_{H,H}$ = 6.9 Hz, C*H*-*i*Pr), 1.33 (3H, d, $^3J_{H,H}$ = 7.0 Hz, CH_3-*i*Pr), 1.28 (3H, d, $^3J_{H,H}$ = 7.0 Hz, CH_3-*i*Pr), 0.86 (3H, d, $^3J_{H,H}$ = 7.1 Hz, CH_3-*i*Pr), 0.73 (3H, d, $^3J_{H,H}$ = 6.8 Hz, CH_3-*i*Pr). ^{13}C{^{1}H} NMR (C$_6$D$_6$, 150 MHz, 295 K): δ 170.0, 160.4, 137.7, 136.4, 135.9, 133.9, 131.7, 131.3, 127.4, 127.2, 126.9, 66.5, 57.7, 48.6, 29.9, 29.6, 22.6, 22.6, 18.2, 17.5.

Structure Determinations. The intensity data for the compounds were collected on a Nonius KappaCCD diffractometer using graphite-monochromated Mo Kα radiation. Data were corrected for Lorentz and polarization effects but not for absorption effects.[42,43]

The structures were solved by direct methods (SHELXS[44]) and refined by full-matrix least-squares techniques against F_o^2 (SHELXL-97[44]). The hydrogen atoms of compounds **2** and **10** and the hydrogen atoms bound to the amide functionalities were located by difference Fourier synthesis and refined isotropically. The other hydrogen atoms were included at calculated positions with fixed thermal parameters. All nondisordered non-hydrogen atoms were refined anisotropically.[44]

Crystallographic data as well as structure solution and refinement details are summarized in Table S1 as part of the Supporting Information. XP (SIEMENS Analytical X-ray Instruments, Inc.) was used for structure representations.

Computational Methods. Full geometry optimizations (i.e., without symmetry constraints) were carried out with the GAUSSIAN 09 program package using throughout the hybrid Hartree−Fock-DFT approach (B3LYP/6-311G(d,p)).[45−47] Stationary points of geometry optimizations were characterized to be minimum structures according to the absence of any imaginary modes by applying second-order derivative calculations. NMR spectra were calculated with the

continuous set of gauge transformations (CSGT) and the gauge-independent atomic orbital (GIAO) methods.[48] Visualization of any calculated properties was performed using the program package GAUSSVIEW.[49]

■ ASSOCIATED CONTENT

Supporting Information

Tables, figures, and CIF files giving crystallographic data of the crystal structure determinations as well as the NMR spectra of the metal anilides. This material is available free of charge via the Internet at http://pubs.acs.org. Crystallographic data (excluding structure factors) have also been deposited with the Cambridge Crystallographic Data Centre as supplementary publication CCDC-888141 for **2**, CCDC-888142 for **3**, CCDC-888143 for **4**, CCDC-888144 for **7**, CCDC-888145 for **8**, CCDC-888146 for **9**, and CCDC-888147 for **10**. Copies of the data can be obtained free of charge on application to the CCDC, 12 Union Road, Cambridge CB2 1EZ, U.K. (e-mail deposit@ccdc.cam.ac.uk).

■ AUTHOR INFORMATION

Corresponding Author

*M.W.: fax, +49 (0) 3641 9-48102; e-mail, m.we@uni-jena.de.

Author Contributions

§These authors contributed equally.

Notes

The authors declare no competing financial interest.

■ ACKNOWLEDGMENTS

We are very grateful to Rainer Beckert and Roman Goy for valuable discussions as well as to the undergraduate student Thomas Gallert for support in the frame of an advanced laboratory course. The infrastructure of our institute was provided by the EU (European Regional Development Fund, EFRE) and the Friedrich Schiller University Jena. Computing time provided by the Ohio Supercomputing Centre, Columbus, OH, is gratefully acknowledged.

■ REFERENCES

(1) (a) Lappert, M.; Protchenko, A.; Power, P.; Seeber, A. *Metal Amide Chemistry*; Wiley: Chichester, U.K., 2009; Chapter 2, pp 7−38. (b) Mulvey, R. E. *Chem. Soc. Rev.* **1998**, *27*, 339−346. (c) Pauer, F.; Power, P. P. In *Lithium Chemistry: A Theoretical and Experimental Overview*; Sapse, A.-M.; Schleyer, P. v. R., Eds.; Wiley-Interscience: New York; 1995; Chapter 9, pp 295−392. (d) Weiss, E. *Angew. Chem., Int. Ed. Engl.* **1993**, *32*, 1501−1523. (e) Collum, D. B. *Acc. Chem. Res.* **1993**, *26*, 227−234. (f) Collum, D. B. *Acc. Chem. Res.* **1992**, *25*, 448−454. (g) Gregory, K.; Schleyer, P. v. R.; Snaith, R. *Adv. Inorg. Chem.* **1991**, *37*, 47−142. (h) Mulvey, R. E. *Chem. Soc. Rev.* **1991**, *20*, 167−209. (i) Schade, C.; Schleyer, P. v. R. *Adv. Organomet. Chem.* **1987**, *27*, 169−278. (j) Setzer, W. N.; Schleyer, P. v. R. *Adv. Organomet. Chem.* **1985**, *24*, 353−451. (k) Lappert, M. F.; Power, P. P.; Sanger, A. R.; Srivastava, R. C. *Metal and Metaloid Amides: Syntheses, Structures, and Physical and Chemical Properties* Ellis Horwood: Chichester, U.K., 1980; Chapter 2, pp 24−44.

(2) (a) Lappert, M.; Protchenko, A.; Power, P.; Seeber, A. *Metal Amide Chemistry*; Wiley: Chicheste, U.K.r, 2009; Chapter 3, pp 39−78. (b) Lappert, M. F.; Power, P. P.; Sanger, A. R.; Srivastava, R. C. *Metal and Metalloid Amides: Syntheses, Structures, and Physical and Chemical Properties*; Ellis Horwood: Chichester, U.K., 1980; Chapter 3, pp 45−67.

(3) Torvisco, A.; O'Brien, A. J.; Ruhlandt-Senge, K. *Coord. Chem. Rev.* **2011**, *255*, 1268−1292.

(4) (a) Westerhausen, M.; Langer, J.; Krieck, S.; Glock, C. *Rev. Inorg. Chem.* **2011**, *31*, 143−184. (b) Westerhausen, M. *Coord. Chem. Rev.* **1998**, *176*, 157−210. (d) Westerhausen, M. *Trends Organomet. Chem.* **1997**, *2*, 89−105.

(5) Utke, A. R.; Sanderson, R. T. *J. Org. Chem.* **1964**, *29*, 1261−1264.

(6) (a) Johns, A. M.; Chmely, S. C.; Hanusa, T. P. *Inorg. Chem.* **2009**, *48*, 1380−1384. (b) Gillett-Kunnath, M. M.; MacLellan, J. G.; Forsyth, C. M.; Andrews, P. C.; Deacon, G. B.; Ruhlandt-Senge, K. *Chem. Commun.* **2008**, 4490−4492. (c) Tang, Y.; Zakharov, L. N.; Kassel, W. S.; Rheingold, A. L.; Kemp, R. A. *Inorg. Chim. Acta* **2005**, *358*, 2014−2022. (d) Kuhlman, R. L.; Vaartstra, B. A.; Caulton, K. G. *Inorg. Synth.* **1997**, *31*, 8. (e) Frankland, A. D.; Lappert, M. F. *J. Chem. Soc., Dalton Trans.* **1996**, 4151−4152. (f) Boncella, J. M.; Coston, C.; Cammack, J. K. *Polyhedron* **1991**, *10*, 769−770. (g) Vaartstra, B. A.; Huffman, J. C.; Streib, W. E.; Caulton, K. G. *Inorg. Chem.* **1991**, *30*, 121−125. (h) Westerhausen, M.; Schwarz, W. *Z. Anorg. Allg. Chem.* **1991**, *606*, 177−190. (i) Westerhausen, M. *Inorg. Chem.* **1991**, *30*, 96−101. (j) Cloke, F. G. N.; Hitchcock, P. B.; Lappert, M. F.; Lawless, G. A.; Royo, B. *J. Chem. Soc., Chem. Commun.* **1991**, 724−726. (k) Hitchcock, P. B.; Lappert, M. F.; Lawless, G. A.; Royo, B. *J. Chem. Soc., Chem. Commun.* **1990**, 1141−1142. (l) Bradley, D. C.; Hursthouse, M. B.; Ibrahim, A. A.; Malik, K. M. A.; Motevalli, M.; Möseler, R.; Powell, H.; Runnacles, J. D.; Sullivan, A. C. *Polyhedron* **1990**, *9*, 2959−2964.

(7) (a) Torvisco, A.; Ruhlandt-Senge, K. *Organometallics* **2011**, *30*, 986−991. (b) Gillett-Kunnath, M.; Teng, W.; Vargas, W.; Ruhlandt-Senge, K. *Inorg. Chem.* **2005**, *44*, 4862−4870. (c) Vargas, W.; Englich, U.; Ruhlandt-Senge, K. *Inorg. Chem.* **2002**, *41*, 5602−5608. (d) Kennedy, A. R.; Mulvey, R. E.; Schulte, J. H. *Acta Crystallogr.* **2001**, *C57*, 1288−1289. See also related $Me_2Si(NDipp)_2Ae(thf)_n$: Yang, D.; Ding, Y.; Wu, H.; Zheng, W. *Inorg. Chem.* **2011**, *50*, 7698−7706.

(8) Gärtner, M.; Fischer, R.; Langer, J.; Görls, H.; Walther, D.; Westerhausen, M. *Inorg. Chem.* **2007**, *46*, 5118−5124.

(9) Glock, C.; Görls, H.; Westerhausen, M. *Inorg. Chem.* **2009**, *48*, 394−399.

(10) Glock, C.; Görls, H.; Westerhausen, M. *Inorg. Chim. Acta* **2011**, *374*, 429−434.

(11) Gärtner, M.; Görls, H.; Westerhausen, M. *Inorg. Chem.* **2007**, *46*, 7678−7683.

(12) Gärtner, M.; Görls, H.; Westerhausen, M. *Dalton Trans.* **2008**, 1574−1582.

(13) (a) Mulvey, R. E. *Acc. Chem. Res.* **2009**, *42*, 743−755. (b) Mulvey, R. E. *Organometallics* **2006**, *25*, 1060−1075. (c) Mulvey, R. E. *Chem. Commun.* **2001**, 1049−1056.

(14) Westerhausen, M. *Dalton Trans.* **2006**, 4755−4768.

(15) Glock, C.; Görls, H.; Westerhausen, M. *Dalton Trans.* **2011**, *40*, 8108−8113.

(16) Glock, C.; Görls, H.; Westerhausen, M. *Chem. Commun.* **2012**, *48*, 7094−7096.

(17) (a) Reznichenko, A. L.; Hultzsch, K. C. *Top. Organomet. Chem.* **2013**, *43*, 51−114. (b) Haag, B.; Mosrin, M.; Ila, H.; Malakhov, V.; Knochel, P. *Angew. Chem., Int. Ed.* **2011**, *50*, 9794−9824. (c) Kobayashi, S.; Yamashita, Y. *Acc. Chem. Res.* **2011**, *44*, 58−71. (d) Harder, S. *Chem. Rev.* **2010**, *110*, 3852−3876. (e) Barrett, A. G. M.; Crimmin, M. R.; Hill, M. S.; Procopiou, P. A. *Proc. R. Soc. London* **2010**, *466*, 927−963. (f) Kazmaier, U. *Angew. Chem., Int. Ed.* **2009**, *48*, 5790−5792. (g) Coles, M. P. *Curr. Org. Chem.* **2008**, *12*, 1220−1230. (h) Müller, T. E.; Hultzsch, K. C.; Yus, M.; Foubelo, F.; Tada, M. *Chem. Rev.* **2008**, *108*, 3795−3892.

(18) Barrett, A. G. M.; Crimmin, M. R.; Hill, M. S.; Hitchcock, P. B.; Lomas, S. L.; Mahon, M. F.; Procopiou, P. A. *Dalton Trans.* **2010**, *39*, 7393−7400.

(19) (a) Wixey, J. S.; Ward, B. D. *Chem. Commun.* **2011**, *47*, 5449−5451. (b) Wixey, J. S.; Ward, B. D. *Dalton Trans.* **2011**, *40*, 7693−7696. (c) Barrett, A. G. M.; Brinkmann, C.; Crimmin, M. R.; Hill, M. S.; Hunt, P.; Procopiou, P. A. *J. Am. Chem. Soc.* **2009**, *131*, 12906−12907. (d) Arrowsmith, M.; Hill, M. S.; Kociok-Köhn, G. *Organometallics* **2009**, *28*, 1730−1738. (e) Buch, F.; Harder, S. *Z. Naturforsch.* **2008**, *63b*, 169−177. (f) Datta, S.; Gamer, M. T.; Roesky, P. W. *Organometallics* **2008**, *27*, 1207−1213. (g) Datta, S.; Roesky, P. W.;

Blechert, B. *Organometallics* **2007**, *26*, 4392−4394. (h) Crimmin, M. R.; Casely, I. J.; Hill, M. S. *J. Am. Chem. Soc.* **2005**, *127*, 2042−2043.
(20) (a) Brinkmann, C.; Barrett, A. G. M.; Hill, M. S.; Procopiou, P. A. *J. Am. Chem. Soc.* **2012**, *134*, 2193−2207. (b) Panda, T. K.; Hrib, C. G.; Jones, P. G.; Jenter, J.; Roesky, P. W.; Tamm, M. *Eur. J. Inorg. Chem.* **2008**, 4270−4279.
(21) Tesh, K. F.; Hanusa, T. P.; Huffman, J. C. *Inorg. Chem.* **1990**, *29*, 1584−1586.
(22) Armstrong, D. R.; Graham, D. V.; Kennedy, A. R.; Mulvey, R. E.; O'Hara, C. T. *Chem. Eur. J.* **2008**, *14*, 8025−8034.
(23) Gärtner, M.; Görls, H.; Westerhausen, M. *Acta Crystallogr., Sect. E* **2007**, *63*, m2289.
(24) Glock, C.; Görls, H.; Westerhausen, M. *Eur. J. Inorg. Chem.* **2011**, 5288−5298.
(25) Gärtner, M.; Görls, H.; Westerhausen, M. *Acta Crystallogr., Sect. E* **2007**, *63*, m2287.
(26) Kennedy, A. R.; Klett, J.; O'Hara, C. T.; Mulvey, R. E.; Robertson, G. M. *Eur. J. Inorg. Chem.* **2009**, 5029−5035.
(27) Westerhausen, M.; Hartmann, M.; Makropoulos, N.; Wieneke, B.; Wieneke, M.; Schwarz, W.; Stalke, D. *Z. Naturforsch.* **1998**, *53b*, 117−125.
(28) Westerhausen, M.; Schwarz, W. *Z. Anorg. Allg. Chem.* **1991**, *604*, 127−140.
(29) Davidson, M. G.; Garcia-Vivo, D.; Kennedy, A. R.; Mulvey, R. E.; Robertson, S. D. *Chem. Eur. J.* **2011**, *17*, 3364−3369.
(30) (a) Chalk, A. J. *Tetrahedron Lett.* **1972**, 3487−3490. (b) Schulte, K. E.; Reisch, J.; Walker, H. *Chem. Ber.* **1965**, *98*, 98−103.
(31) Ramanathan, B.; Keith, A. J.; Armstrong, D.; Odom, A. L. *Org. Lett.* **2004**, *6*, 2957−2960.
(32) Chalk, A. J. *Tetrahedron* **1974**, *30*, 1387−1391.
(33) According to Houser and co-workers, the simple four-coordinate geometry index τ_4 allows determination of the geometry of tetracoordinate atoms by applying the equation $\tau_4 = [360° - (\alpha + \beta)]/141°$, with α and β being the largest angles. Values of 1 and 0 for τ_4 are obtained for ideal tetrahedral and square-planar environments, respectively, whereas 0.85 and values between 0.07 and 0.64 are symptomatic of trigonal-pyramidal and seesaw geometries, respectively. For C1 in compound **10** this concept gives a value of $\tau_4 = 0.88$. For further details see: Yang, L.; Powell, D. R.; Houser, R. P. *Dalton Trans.* **2007**, 955−964.
(34) (a) Matzinger, S.; Bally, T. *J. Phys. Chem. A* **2000**, *104*, 3544−3552. (b) McMahon, R. J.; Abelt, C. J.; Chapman, O. L.; Johnson, J. W.; Kreil, C. L.; LeRoux, J.-P.; Mooring, A. M.; West, P. R. *J. Am. Chem. Soc.* **1987**, *109*, 2456−2469. (c) West, P. R.; Chapman, O. L.; LeRoux, J.-P. *J. Am. Chem. Soc.* **1982**, *104*, 1779−1782.
(35) (a) Mahlokozera, T.; Goods, J. B.; Childs, A. M.; Thamattoor, D. M. *Org. Lett.* **2009**, *11*, 5095−5097. (b) Kassaee, M. Z.; Azarnia, J.; Arshadi, S. *J. Mol. Struct. (THEOCHEM)* **2004**, *686*, 115−122. (c) Matzinger, S.; Bally, T.; Patterson, E. V.; MacMahon, R. J. *J. Am. Chem. Soc.* **1996**, *118*, 1535−1542. (d) Schreiner, P. R.; Karney, W. L.; Schleyer, P. v. R.; Borden, W. T.; Hamilton, T. P.; Schaefer, H. F. *J. Org. Chem.* **1996**, *61*, 7030−7039. (e) Wong, M. E.; Wentrup, C. *J. Org. Chem.* **1996**, *61*, 7022−7029. (f) Waali, E. E. *J. Am. Chem. Soc.* **1981**, *103*, 3604−3606.
(36) Wang, X.; Yang, Z.; Wang, J.; Zhang, J.; Cao, W. *J. Mol. Struct. (THEOCHEM)* **2006**, *766*, 169−175.
(37) Santos, J. C.; Andres, J.; Aizman, A.; Fuentealba, P.; Polo, V. *J. Phys. Chem. A* **2005**, *109*, 3687−3693.
(38) Alabugin, I. V.; Kovalenko, S. V. *J. Am. Chem. Soc.* **2002**, *124*, 9052−9053.
(39) Lavy, S.; Pérez-Luna, A.; Kündig, E. P. *Synlett* **2008**, 2621−2624.
(40) Norizuki, Y.; Komano, K.; Sato, I.; Hirama, M. *Chem. Commun.* **2008**, 5372−5374.
(41) Clark, A. E.; Bhattacharryya, S.; Zaleski, J. M. *Inorg. Chem.* **2009**, *48*, 3926−3933.
(42) *COLLECT, Data Collection Software*; Nonius BV, Rotterdam, The Netherlands, 1998.
(43) Otwinowski, Z.; Minor, W. Processing of X-Ray Diffraction Data Collected in Oscillation Mode. In *Methods in Enzymology*; Carter, C. W., Sweet, R. M., Eds.; Academic Press: New York, 1997; Vol. *276* (Macromolecular Crystallography, Part A), pp 307−326.
(44) Sheldrick, G. M. *Acta Crystallogr.* **2008**, *A64*, 112−122.
(45) Frisch, M. J.; Trucks, G. W.; Schlegel, H. B.; Scuseria, G. E.; Robb, M. A.; Cheeseman, J. R.; Scalmani, G.; Barone, V.; Mennucci, B.; Petersson, G. A.; Nakatsuji, H.; Caricato, M.; Li, X.; Hratchian, H. P.; Izmaylov, A. F.; Bloino, J.; Zheng, G.; Sonnenberg, J. L.; Hada, M.; Ehara, M.; Toyota, K.; Fukuda, R.; Hasegawa, J.; Ishida, M.; Nakajima, T.; Honda, Y.; Kitao, O.; Nakai, Y.; Vreven, T.; Montgomery, J. A., Jr.; Peralta, J. E.; Ogliaro, F.; Bearpark, M.; Heyd, J. J.; Brothers, E.; Kudin, K. N.; Staroverov, V. N.; Kobayashi, R.; Normand, J.; Raghavachari, K.; Rendell, A.; Burant, J. C.; Iyengar, S. S.; Tomasi, J.; Cossi, M.; Rega, N.; Millam, J. M.; Klene, M.; Knox, J. E.; Cross, J. B.; Bakken, V.; Adamo, C.; Jaramillo, J.; Gomperts, R.; Stratmann, R. E.; Yazyev, O.; Austin, A. J.; Cammi, R.; Pomelli, C.; Ochterski, J. W.; Martin, R. L.; Morokuma, K.; Zakrzewski, V. G.; Voth, G. A.; Salvador, P.; Dannenberg, J. J.; Dapprich, S.; Daniels, A. D.; Farkas, O.; Foresman, J. B.; Ortiz, J. Cioslowski, J. V.; Fox, D. J. *Gaussian 09, Revision A.01*; Gaussian, Inc., Wallingford, CT, 2009.
(46) Becke, A. D. *J. Chem. Phys.* **1993**, *98*, 5648−5652.
(47) Lee, C.; Yang, W. W.; Parr, P. R. *Phys. Rev.* **1988**, *B37*, 785−789.
(48) Cheeseman, J. R.; Trucks, G. W.; Keith, T. A.; Frisch, M. J. *J. Chem. Phys.* **1996**, *104*, 5497−5509.
(49) Dennington II, R. D.; Keith, T. A.; Millam, J. A. *GAUSSVIEW 5.0*; Gaussian, Inc., Wallingford, CT, 2000.